

Charge exchange processes with emission of secondary excited silicon ions

D. V. Ledyankin, I. F. Urazgil'din, and V. E. Yurasova

Moscow State University

(Submitted 27 April 1988)

Zh. Eksp. Teor. Fiz. **94**, 90–100 (December 1988)

The features of electron exchange between secondary excited silicon ions and an Si (111) surface are investigated experimentally and theoretically. It is determined that when the energy of the excited ion level is near the maxima of the surface electron state density the energy spectrum of Si^{+*} manifests an oscillatory nature due to charge exchange. It is demonstrated that the experimentally observed oscillations can be explained if it is assumed that electron exchange within the solid occurs prior to the passage of the ion through the surface.

1. INTRODUCTION

The oscillatory nature of the energy and angular distributions of excited silicon ions resulting from the bombardment of a silicon surface by 7.5 keV Ne^+ ions was detected in Ref. 1. This effect has been qualitatively attributed to quasiresonant charge exchange between the excited ion and the levels of the surface electron states of silicon. Similar oscillations have also been observed in experiments on He^+ ion scattering on a number of metallic surfaces from changes in the primary particle energies.^{2,3} These oscillations are related to quasiresonant vibrational electron exchange between the energy level of the atomic shells of the solid and the ground state of the scattered particle.⁴

In spite of the similar nature of the energy distribution of scattered ions and secondary excited ions there are significant differences in the physical processes responsible for the features of these distributions, particularly the processes behind electron exchange. The present study carried out a theoretical and experimental investigation of the energy distributions for different excited states of secondary silicon ions, which made it possible to draw certain conclusions regarding the formation mechanism of the charge state.

2. EXPERIMENTAL TECHNIQUE

A multichannel device with a coincidence circuit was developed in order to simultaneously analyze the emission of the secondary particles (ions, photons and electrons) resulting from the ion bombardment of a solid. This apparatus can be used to obtain information on the energy and angular dependence of the detachment of the various particle types from the bombardment region and to distinguish in time the elementary particle interaction events.

A block diagram of the assembly is shown in Fig. 1. A Von Ardenne duoplasmatron was used as the ion source (1); this unit made it possible to obtain an ion beam (Ar^+ and Ne^+) of 4 to 8 keV and a current density at the specimen of $150\text{--}300\ \mu\text{A}/\text{cm}^2$, which provided dynamic surface cleaning at $P = 5 \cdot 10^{-7}$ torr. The manipulator (2) made it possible to control the angle of ion beam incidence on the specimen. A spherical electrostatic analyzer (3) with energy resolution of $E/\Delta E = 100$ was employed as the secondary charge particle energy analyzer. The energy analyzer could be rotated about the target bombardment region. The photon recording channel consisted of a quartz window (4), a quartz lens (5), and an interference filter (6); the optical axis was parallel to the specimen surface and perpendicular to the bombardment plane. Secondary ions and photons were collected

in solid angles of $5 \cdot 10^{-5}$ and $1 \cdot 10^{-4}$ steradian, respectively. The measurement system consisted of two symmetrical channels including a detector: A channel electron multiplier (7) or a photomultiplier (8), a pulsed amplifier (9, 10), controlled delay lines (11, 12) and pulse shapers (13, 14). The shaper signals from the separate channel were sent to a coincidence circuit (15). If the discrepancy in the arrival time of the pulse was less than the resolution of the coincidence circuit, the circuit sent a pulse of the scalar (16); the presence of a pulse indicated that two particles were registered simultaneously.

The transit time of particles of specific masses and energies was calculated in the course of the experiment; the difference in the arrival time for a recorded particle pair was cancelled by introducing an equivalent delay into the fast particle recording channel. Note that in order to accurately determine the number of created particles, no more than a single elementary particle formation event can be recorded over the resolution time of the coincidence circuit ($\tau = 50$ nsec). This condition was satisfied in our experiments. The number of coincidences over a specific time after subtraction of the background of random coincidences will be given below.

A silicon monocrystal, (111) face, was used as the specimen. The specimen was thermally outgassed at 550°C for 1 hour and simultaneously cleaned by an Ar^+ ion beam at a current density $200\ \mu\text{A}/\text{cm}^2$ in the measurement

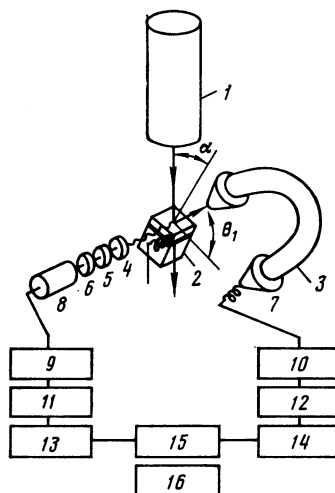


FIG. 1. Block diagram of the apparatus.

chamber. The specimen was heated to 350 °C during the experiment to prevent amorphization. This was confirmed by the anisotropy of the angular dependence of Si⁺ ion emission. The specimen was bombarded at different angles to the surface by 8 keV Ne⁺ and Ar⁺ ions. The beam current density was 150 μA/cm² with a residual gas pressure of 5 · 10⁻⁷ torr. The photons were observed in different directions in the bombarded Si (111) plane. Any change in the observation angle in this plane had no qualitative effect on the observed relations, but rather altered only the photon radiation intensity. Secondary Si⁺ ions of a specific energy was recorded along the normal to the specimen surface or at the angle θ_i = 40° from the normal, near the [110] direction.

The number of formation time coincidences of secondary Si⁺ silicon ions and photons of different wavelengths (arriving from the decay of the excited state of the Si²⁺ ion) was measured as a function of the energy of the secondary Si⁺ ion; i.e., the energy spectrum of the secondary excited ions was essentially the subject of investigation. The measurements were carried out for different Si II lines at λ = 385.6, 413 and 567 nm associated with the decay of the excited Si²⁺ 4p(2P_{3/2}^o); Si²⁺ 4f(2F_{5/2}^o) and Si²⁺ 4p(4D) states, respectively.

3. ENERGY DISTRIBUTION FOR Si²⁺ 4p(2P_{3/2}^o)

3.1. Experiment and discussion

The energy distribution of the excited Si²⁺ 4p(2P_{3/2}^o) ions was investigated for the case of bombardment of the (111) face of Si by 8 keV Ar⁺ ions incident near the normal to the surface (α ~ 8°). The secondary Si⁺ ions were observed at θ_i = 40° from the normal, while the photons were observed in the [110] direction parallel to the surface.

Figure 2 shows the number of coincidences of secondary Si⁺ ions and photons at λ = 385.6 nm as a function of the Si⁺ energy (i.e., the energy distribution of the Si²⁺ 4p(2P_{3/2}^o) ion; the decay of the excited state of this ion causes emission at λ = 385.6 nm). If this oscillating energy distribution is plotted as a function of v_⊥⁻¹, where v_⊥ is the ion velocity component perpendicular to the surface, the oscillation period will remain constant. The constancy of the intensity oscillation period as a function of v⁻¹ is characteristic of the resonant charge exchange processes from particle collisions.⁶ In our case the decisive role of v_⊥ suggests that the secondary ion interacts with the solid surface, and does not have a binary character. We will consider a possible electron exchange process that could explain the observed oscillations in the energy spectrum.

Analysis of the electron structure of silicon (Fig. 3)

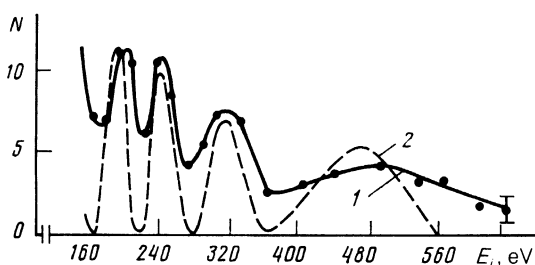


FIG. 2. Number of coincidences of secondary Si⁺ ions and photons at λ = 385.6 nm over 100 sec plotted as a function of Si⁺ energy (curve 1: Experiment; curve 2: Calculation).

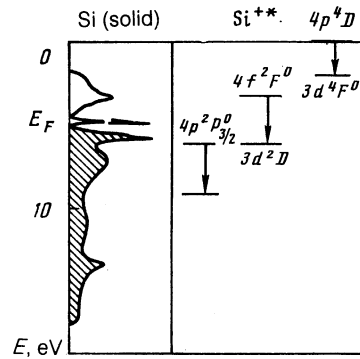


FIG. 3. Electron structure of silicon and electron transition scheme in Si²⁺.

demonstrates that a peak of the surface electron states with E = 5.9 eV⁷ exists near the excited level of the ion at E = 6.3 eV responsible for radiation of the Si II line at λ = 385.6 nm; this peak is near the Fermi level, and the surface layer of silicon atoms makes the primary contribution to the Fermi level. We note that the distribution of the peaks of the surface states is fairly stable under the Si(2 × 1) → Si(7 × 7) surface reconstruction which occurs when the specimen is heated.⁸ Electron exchange may occur between the excited level of the Si²⁺ ion and the narrow peak of the surface states.

When oxygen is admitted to the measurement chamber, the peak of the electron states diminishes near the Fermi level. This will violate the charge exchange conditions and will cause the oscillating nature of Si²⁺ detachment to vanish, which was in fact observed in experiment (Fig. 4).

The electron exchange mechanism responsible for the spectrum shown in Fig. 2 can therefore be explained as follows. Vacancies form in the deep L-shell of silicon from the bombardment of the silicon surface by Ar⁺ and Ne⁺ ions due to Si-Si and Ar-Si hard collisions, as supported by an analysis of the correlation diagrams.⁹ A doubly-charged Si²⁺ ion forms the Auger process involving the outer L-shells. Charge exchange with the surface silicon levels then produces Si²⁺ 4p(2P_{3/2}^o) whose decay yields Si⁺ ions and photons that are simultaneously in our experiment.

The following experiment was conducted to identify the role of the Auger process in the formation of the secondary excited ions. The number of coincidences of the Auger electron with Si II photons at λ = 385.6 nm was measured as a

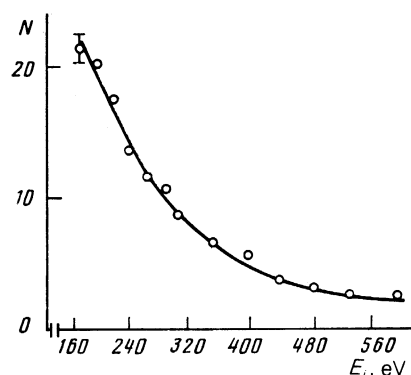


FIG. 4. Number of coincidences of secondary Si⁺ ions and photons at λ = 385.6 nm over 30 sec for an oxidized surface of the silicon specimen.

function of the delay in the photon emission channel.

The maximum number of coincidences corresponds to electrons of energy $E_e = 86$ eV. Consequently the formation of at least some of the Si^{+*} ions is accompanied by the emission of Auger electrons of energy $E_e = 86$ eV. However the ion state of interest to us can form by means of the Auger process at such an electron energy only within the solid, i.e., by the LVV -transition (an electron of an entirely different energy corresponds to the LMM -transition which occurs outside the solid). Consequently we believe that a reasonable conclusion is that the LVV -transition precedes the formation of the $\text{Si}^{+*} 4p(^2P_{3/2}^0)$ state. Under ion bombardment of the surface the Auger processes within the solid (LVV) may occur at a higher intensity than outside the solid (LMM).¹⁰

This analysis therefore allows us to make an important assumption in our study: The Si^{2+} ions form within the solid before passing through the surface.

3.2. Theoretical analysis

According to the preceding analysis the oscillatory nature of the energy distribution of excited $\text{Si}^{+*} 4p(^2P_{3/2}^0)$ ions (Fig. 2) can be attributed to the features of electron exchange between the excited level of the Si^{+*} ion and the narrow peak of the surface states. This peak can be described as a discrete electron level.⁴ In this case the analysis can be carried out for a two-level electron charge exchange model. A detailed presentation of such models can be found in Refs. 11, 12. We will use the Demkov model¹³ and will retain the same notation for convenience.

We will roughly represent the wave function of the system as $\Psi = a(t)\Psi_A + b(t)\Psi_B$, where Ψ_A, Ψ_B are the wave functions of the electron in the states associated with the surface and the ion, respectively. The following system of equations is obtained for the coefficients $a(t), b(t)$ in this approximation (here and henceforth we will use the atomic system of units: $\hbar = m = e = 1$)

$$i\dot{a} = H_{11}a + H_{12}b, \quad i\dot{b} = H_{21}a + H_{22}b, \quad (1)$$

where H_{ik} are certain functions of the distance $R(t)$ from the ion to the surface layer of the atoms. The quantities $a(t)$ and $b(t)$ determine the probabilities $\omega_1 = |a|^2$ and $\omega_2 = |b|^2$ of the electron being in the corresponding states.

We will assume that H_{11} and H_{22} are independent of R , i.e., $H_{11} = -E_A, H_{22} = -E_B$, where E_i is the energy of the levels of interest to us. The exchange term H_{12} is expressed through the integral containing the functions Ψ_A and Ψ_B and, consequently, decreases exponentially as $|R| \rightarrow \infty, H_{12} = H_0 \exp[-(2E_0)^{1/2}|R|]$, where E_0 is the lower energy of states A and B . If Eqs. (1) are integrated with the initial conditions $|a(-t_0)| = 1, b(-t_0) = 0$ (which will be discussed below), the quantity $\omega = |b(\infty)|^2$ will determine the charge exchange probability. The nature of the solution is essentially dependent on the ratio between the magnitude of the resonance defect $\Delta = H_{11} - H_{22}$ and the exchange term H_{12} . The Demkov model assumes that the system passes through five regions during development: $\Delta > H_{12}, \Delta \sim H_{12}, \Delta < H_{12}, \Delta \sim H_{12}, \Delta > H_{12}$. The nature of the molecular wave functions changes in region R_0 , where we have $H_{12} \sim \Delta$, i.e., the nonadiabatic transitions occur specifically in this region, and outside this region the system develops adiabatically. The charge exchange probability deter-

mined by Eqs. (2) with the initial conditions $|a(-\infty)| = 1, b(-\infty) = 0$ takes the following form¹³

$$\omega = |b(\infty)|^2 = \text{sech}^2 \frac{\pi\Delta}{2^{1/2}E_0^{1/2}} \left| \frac{dR}{dt} \right|^{-1} \sin^2 \int_{R_0}^{\infty} H_{12}(t) dt, \quad (2)$$

or, assuming in fixed velocity:

$$\omega = \text{sech}^2 \frac{\pi\Delta}{2^{1/2}E_0^{1/2}v} \sin^2 \frac{2}{v} \int_0^{\infty} H_{12}(R) dR. \quad (3)$$

In order to determine the value of ω it is necessary to know the value of the exchange integral H_{12} , which in this case can be used as a fitting parameter. The best agreement with the experimental data is obtained for $H_0 = 0.12$ (Fig. 2), which is quite realistic for our situation when H_{11} and H_{22} are independent of R . The energy distribution of Si^{+*} (Fig. 2, curve 2) is the product of the charge exchange probability ω and the corresponding cross section $\sigma(E)$, which has a monotonically diminishing dependence on E (in the range of energies characteristic of our experiment we find $\sigma(E) \propto E^{-1}$). For the adiabatic transition region where $H_{12} \sim \Delta$ ($\Delta = 0.4$ eV), we obtain $R_0 = 1.5-2$ Å, which remains virtually constant for the velocities characteristic of the experiment ($v = 0.01-0.03$), which also follows from Ref. 14. Consequently the system will begin to develop at distances to the surface $R(t)$ greater than the value of R_0 obtained (the region $\Delta > H_{12}$), which assumes that the initial state of the Si^{2+} ($b(-t_0) = 0$) ion must arise prior to the distance R_0 .

The selection of the initial conditions for solving Eqs. (1) is dictated by the fact that, as discussed in the preceding section, the Si^{2+} ion forms within the solid (rather than upon detachment from the surface), as represented by the initial condition $b(-t_0) = 0$ (no electron on an excited level prior to the charge exchange process). The condition $a(-t_0) = 1$ corresponds to a filled peak of the surface state density below the Fermi level.

It is important to note that the LVV Auger process occurring inside the solid can directly result in the formation of the $\text{Si}^{+*} 4p(^2P_{3/2}^0)$ excited state under analysis. Then the

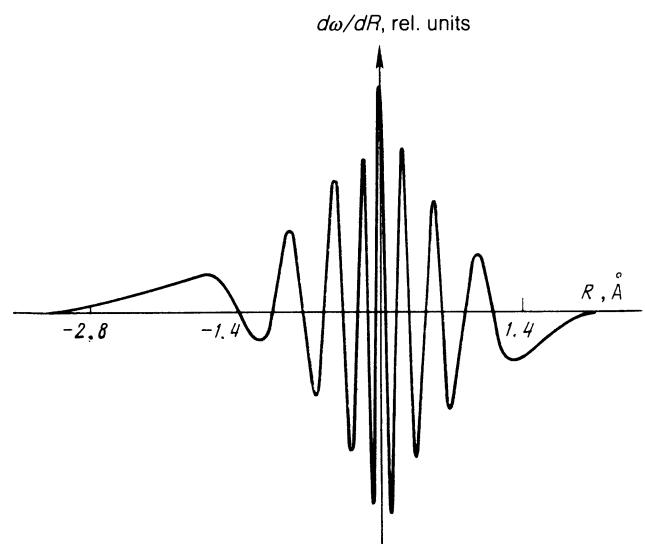


FIG. 5. Variation in the charge exchange probability of secondary Si^{+*} ions at $E = 114$ eV plotted as a function of distance to the surface.

problem is reduced to determining the probability p of the conservation of this state after charge exchange, although with a different peak of the electron state density above the Fermi level ($E = 4.9$ eV). However in this energy range the probability $p = 1 - \omega$ is very near 1 in practice, since ω becomes negligible due to the substantial growth of $\Delta = 1.4$ eV in the exponential term $\text{sech}^2 [\pi\Delta/2^{3/2}E_0^{1/2}v]$ in (3). Consequently such an Si^{**} formation channel will not cause oscillations in the energy spectrum, and will only be capable of altering the overall level. Analysis of the charge exchange process within the framework of this model allows certain estimates. Figure 5 plots the change in charge exchange probability of secondary Si^{**} ions as a function of the distance to the surface, i.e., $d\omega/dR = f(R)$. This relation indicates, specifically, that the final charge state of an escaping particle will form at $< 3 \text{ \AA}$ from the surface.

4. ENERGY DISTRIBUTION FOR $\text{Si}^{**} 4f(2F^0)$

4.1. Experiment

The energy spectrum of $\text{Si}^{**} 4f(2F^0)$ ions was investigated by bombarding $\text{Si}(111)$ faces with 8 keV Ar^+ ions incident at 40° with respect to the normal to the surface in a high-index direction that eliminates channelling [10° from $[110]$ in the (100) plane]. The secondary ions were observed along the normal to the surface, while the photons were observed in the $[110]$ direction parallel to the (111) surface.

Figure 6 shows the number of coincidences of secondary Si^+ ions and photons at $\lambda = 413$ nm as a function of the secondary Si^+ ion energy. Photons at $\lambda = 413$ nm are radiated due to the decay of the excited $\text{Si}^{**} 4f(2F^0)$ state. The spectrum is identical to that of the $\text{Si}^{**} 4p(2P_{3/2}^0)$ state, which has an oscillatory nature. The energy of the excited $\text{Si}^{**} 4f(2F^0)$ level is 3.5 eV (from the vacuum level). Figure 3 clearly indicates that this energy is significantly less than the energy of the surface peak of the electron state density

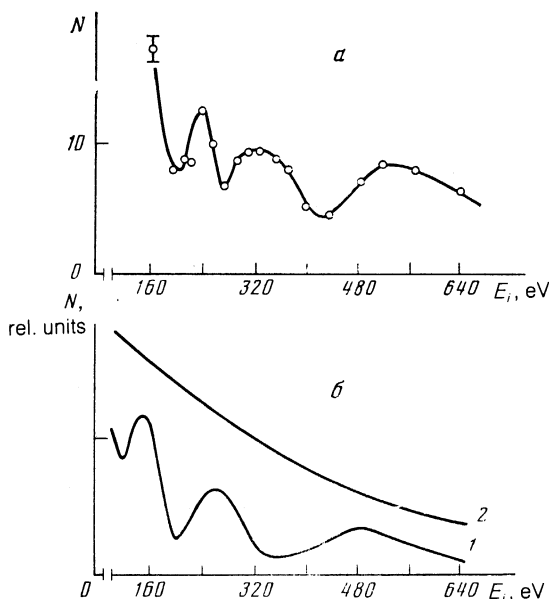


FIG. 6. a—Number of coincidence of secondary Si^+ ions and photons at $\lambda = 413$ nm over 30 sec plotted as a function of secondary Si^+ ion energy; b—same: Calculation: Curve 1 for the function $u_1(t)$, curve 2 for the function $u_2(t)$.

and lies in the energy range of the conduction band electrons. It is therefore reasonable to attempt to attribute oscillations in the energy spectrum of $\text{Si}^{**} 4f(2F^0)$ to the features of electron exchange between the secondary Si^{**} ion and the conduction band of silicon.

4.2. Theory

We proceed to a theoretical treatment of the energy spectrum of excited $\text{Si}^{**} 4f(2F^0)$ ions. In this case the two-level approach analogous to that examined in Sec. 3.2 is not suitable due to the lack of a clearly-expressed peak of the energy state density in an energy range near the energy of this excited level. It becomes necessary to calculate charge exchange with a set of surface silicon levels. An Anderson-Newns Hamiltonian can be used to solve this class of problems^{15,16}

$$H(t) = H_0(t) + V(t), \quad (4)$$

$$H_0(t) = E_a C_a + C_a + \sum_k E_k C_k + C_k, \quad (5)$$

$$V(t) = \sum_k (V_{ak}(t) C_k + C_a + V_{ka}^*(t) C_a + C_k), \quad (6)$$

where H_0 is the Hamiltonian of the ion/crystal system without interaction between the subsystems; C_a , C_k and C_a^+ , C_k^+ are the electron destruction and creation operators in the state associated with the ion Ψ_a or crystal Ψ_k , respectively; Ψ_a and Ψ_k is the complete orthogonal system of eigenfunctions of the Hamiltonian H_0 with the eigenvalues E_a and E_k . The operator $V(t)$ represents exchange interaction between the states Ψ_a and Ψ_k , V_{ak} are the matrix elements of $\langle \Psi_a | V(t) | \Psi_k \rangle$. Coulomb repulsion and electron spin are ignored, and E_a and E_k are assumed to be independent of time, which is entirely legitimate for a semiconductor.

Thus the Schrödinger equation with Hamiltonian (4) is considered:

$$i \frac{\partial \Psi(x, t)}{\partial t} = H \Psi(x, t). \quad (7)$$

It is advisable to go over to the interaction representation, i.e., to seek the wave function as

$$\Psi(x, t) = \exp(-iH_0 t) \Phi(x, t). \quad (8)$$

Substituting (8) into (7) and using (4) we obtain

$$i \frac{\partial \Phi(x, t)}{\partial t} = \mathcal{V}(t) \Phi(x, t), \quad (9)$$

where

$$\mathcal{V}(t) = \exp(iH_0 t) V(t) \exp(-iH_0 t).$$

We expand the wave function $\Phi(x, t)$ in the eigenfunctions of the operator H_0 .

$$\Phi(x, t) = \sum_i b_i(t) \Psi_i(x); \quad (10)$$

here $|b_i|^2$ is the probability of the electron being in the corresponding state. We substitute (10) into (9), multiplying the left and right sides of the relation from the left by $\Psi_i^*(x)$ and, integrating over the entire range of variation of x , we obtain:

$$i \frac{\partial b_a}{\partial t} = \sum_k \mathcal{V}_{ak} b_k, \quad (11)$$

$$i \frac{\partial b_k}{\partial t} = \sum_j \mathcal{V}_{kj} b_j = \mathcal{V}_{ka} b_a. \quad (12)$$

We assume zero temperature and hence all energy levels above the Fermi level E_F are free, i.e., $b_k(t_0) = 0$. We then obtain from (12)

$$b_k = -i \int_{t_0}^t \mathcal{V}_{ka}(t') b_a(t') dt', \quad (13)$$

while subject to (13) we find from (11)

$$\frac{\partial b_a}{\partial t} = - \sum_k \mathcal{V}_{ak}(t) \int_{t_0}^t \mathcal{V}_{ka}(t') b_a(t') dt'. \quad (14)$$

It is easily shown that

$$\mathcal{V}_{nm}(t) = V_{nm}(t) \exp[it(E_n - E_m)].$$

Hence

$$\frac{\partial b_a}{\partial t} = - \int_{t_0}^t \sum_k V_{ak}(t) V_{ka}^*(t') b_a(t') \exp[i(E_a - E_k)(t - t')] dt'. \quad (15)$$

Following Ref. 15, 16 we assume that the nature of the time dependence is identical for all V_{ij} : $V_{ij}(t) = V_{ij} u(t)$. Then (15) becomes

$$\begin{aligned} \frac{\partial b_a}{\partial t} = & - \int_{t_0}^t u(t) u(t') b_a(t') \exp[iE_a(t - t')] \\ & \times \sum_k |V_{ak}|^2 \exp[-iE_k(t - t')] dt'. \end{aligned}$$

With large k it is natural to go from summation to integration, i.e.,

$$\sum_k |V_{ak}|^2 \exp[-iE_k(t - t')] = \int_{-\infty}^{\infty} \rho(E) \exp[-iE(t - t')] dE,$$

where $\rho(E)$ is the electron state density in the conduction band.¹⁷ We therefore finally have a linear integrodifferential equation for determining the population probability of level E_a :

$$\begin{aligned} \frac{\partial b_a}{\partial t} = & - \int_{t_0}^t u(t) u(t') b_a(t') \exp[iE_a(t - t')] \\ & \times \int_{-\infty}^{\infty} \rho(E) \exp[-iE(t - t')] dE dt' \end{aligned} \quad (16)$$

with the initial condition $b_a(t_0) = 1$, assuming that initially the electron is in the state associated with the ion. The function $u(t)$ is given as follows^{15,16}: $u(t) = u_0 \exp(-\lambda |R|)$, $R = vt$, where v is ion velocity while $\lambda = (2E_0)^{1/2}$; since $\lambda = 1/R_a$,¹³ where R_a is the radius of the corresponding shell, we have $u = u_0(-|R|/R_a)$.

The form of the function $u(t)$ which, as noted above, determines the nature of the time dependence of the interaction energy between the level E_a and the conduction band

levels, is fundamental in this model. We will consider two cases:

- 1) $u_1(t) = u_0 \exp(-\lambda |R|)$;
- 2) $u_2(t) = \begin{cases} u_0, & R < 0, \\ u_0 \exp(-\lambda |R|), & R \geq 0. \end{cases}$

The range $R < 0$ is within the solid, $R \geq 0$ is outside the solid.

The first case assumes that as the ion travels up through the solid to the surface and during subsequent emission, interaction with the surface state is maximized in the surface region ($R = 0$). The second case assumes constant interaction within the solid and a decay of this interaction only upon emission from the surface, i.e., this eliminates the difference between the form of the electron state density on the surface of the solid and in the solid bulk. Equation (16) was solved numerically. The probability $|b_a(t)|^2$ was calculated as $t \rightarrow \infty$, i.e., at a substantial distance from the surface when charge exchange ceases by design for each ion energy (velocity) value in the range of interest to us [the velocity enters into (16) as a parameter].

The use of $u_1(t)$ causes the oscillating form of the energy spectrum of Si^{+*} (Fig. 6, b, curve 1) which corresponds well to experiment, while the use of $u_2(t)$ yields a monotonic form of the energy spectrum (curve 2). The oscillatory nature of the probability of an electron existing on the level under consideration as a function of ion energy and, therefore, the oscillatory form of the energy spectrum is related to the surface localization of interaction [the distribution $\rho(E)$ used here is produced by the surface layers of silicon atoms¹⁷]. The oscillatory nature of the relation is characteristic of quaresonant electron exchange processes⁶ and is related to the interference of the wave functions of the different states.

The excellent qualitative agreement between the experimental and theoretical energy spectra suggest that the experimentally observed oscillations are associated with quaresonance charge exchange between the excited state of the ion and the surface states in the conduction band.

5. ENERGY DISTRIBUTION FOR $\text{Si}^{+*} 4p(^4D)$

The coincidence of secondary Si^+ ions of various energies and photons at $\lambda = 567$ nm resulting from the decay of the excited $\text{Si}^{+*} 4p(^4D)$ state at an energy level 0.05 eV from the vacuum level was determined. The result is shown in Fig.

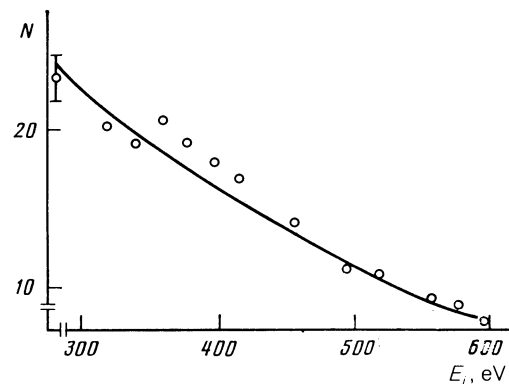


FIG. 7. Number of coincidences of secondary Si^+ ions and photons at $\lambda = 567$ nm over 300 sec as a function of Si^+ energy.

7 which clearly demonstrates that no oscillations in the energy spectrum of the excited Si^{++} ions were observed here.

The energy spectrum of the excited state of the $\text{Si}^{++} 4p(^4D)$ ion ($\lambda = 567 \text{ nm}$) (Fig. 7) can, in view of its monotonic nature, be explained within the framework of the same approach as in the preceding section. However the initial condition of the problem which assumes that such a state develops within the solid, is not valid in this case due to the large radius of the excited ion.

It is therefore possible to assume that the Auger process responsible for the formation of this state occurs outside the solid when $R \geq 0$. Mathematically the problem is reduced to a solution of the same equation (16), although with a different initial condition. The solution depends on the distance from the surface over which the excited state was formed, although the energy spectrum is always monotonic, similar to the spectrum obtained in the preceding section using $u_2(t)$ (Fig. 6, b, curve 2).

6. CONCLUSION

The oscillatory nature of the energy spectrum of excited secondary $\text{Si}^{++} 4p(^2P_{3/2}^0)$, $\text{Si}^{++} 4f(^2F_{5/2}^0)$ ions was observed experimentally for the case of bombardment of a silicon surface with Ar^+ and Ne^+ ions.

A physical model based on the electron exchange between the excited level of the ion and the surface states of silicon has been proposed; this model makes it possible to explain the observed behavior.

It is demonstrated that the oscillatory nature of the spectrum occurs when the exchange process begins within the solid. When the initial state of the ion is formed outside the solid the model yields a monotonic energy spectrum, which is confirmed experimentally by an investigation of the $\text{Si}^{++} 4p(^4D)$ state.

Analysis of the experimental and theoretical data yield a characteristic distance $\leq 3 \text{ \AA}$ from the surface as the range in which the final charge state of the escaping particle is established.

The influence of a change in the electron surface structure (using oxidation as an example) on the nature of the energy spectrum of secondary excited particles has been demonstrated; this can be used in developing surface diagnostic techniques.

¹V. A. Abramenko, D. V. Ledyankin, I. F. Urazgil'din and V. E. Yurasonova, *Pis'ma Zh. Eksp. Teor. Fiz.* **44**, 398 (1986) [*JETP Lett.* **44**, 512 (1986)].

²R. L. Erickson and D. P. Smith, *Phys. Rev. Lett.* **34**, 297 (1975).

³T. W. Rusch and R. L. Erickson, *J. Vac. Sci. Technol.* **13**, 374 (1976).

⁴J. C. Tully, *Phys. Rev. B* **16**, 4324 (1977).

⁵G. A. Dubski, V. G. Neudachin, N. M. Persiantseva *et al.*, *Poverkhnost'*, No. 1, 64 (1985).

⁶J. C. Tully and N. H. Tolk, *Inelastic Ion-Surface Collisions*. Eds. N. H. Tolk *et al.* N.Y. Acad. Press, 1977.

⁷S. Ciraci, B. Butz, E. M. Oellig and H. Wagner, *Phys. Rev. B* **30**, 711 (1984).

⁸P. P. Auer and W. Monch, *Japan J. Appl. Phys. Suppl. 2*, Pt. 2, 397 (1974).

⁹M. Barat and W. Lichten, *Phys. Rev. A* **6**, 211 (1972).

¹⁰C. Benazeth, N. Benazeth and M. Hou, *Surf. Sci.* **151**, L137 (1985).

¹¹E. E. Nikitin and S. Ya. Umanski, *Theory of slow atomic collision*, Springer (1984), Atomizdat, Moscow (1979), p. 277.

¹²V. M. Galitskiy, E. E. Nikitin and B. M. Smirnov, *Atomic particle collision theory*, Nauka, Moscow, (1981), p. 54.

¹³Yu. N. Demkov, *Pis'ma Eksp. Teor. Fiz.* **45**, 195 (1963) [*JETP Lett.* **45**, (1963)].

¹⁴M. R. Spalburg, J. Los and A. Z. Devdariani, *Chem. Phys.* **103**, 253 (1986).

¹⁵W. Bloss and D. Hone, *Surf. Sci.* **72**, 277 (1978).

¹⁶R. Brako and D. M. News, *Surf. Sci.* **108**, 253 (1981).

¹⁷Qian Guo-Xin and D. J. Chadi, *Phys. Rev. B* **35**, 1288 (1987).

Translated by Kevin S. Hendzel